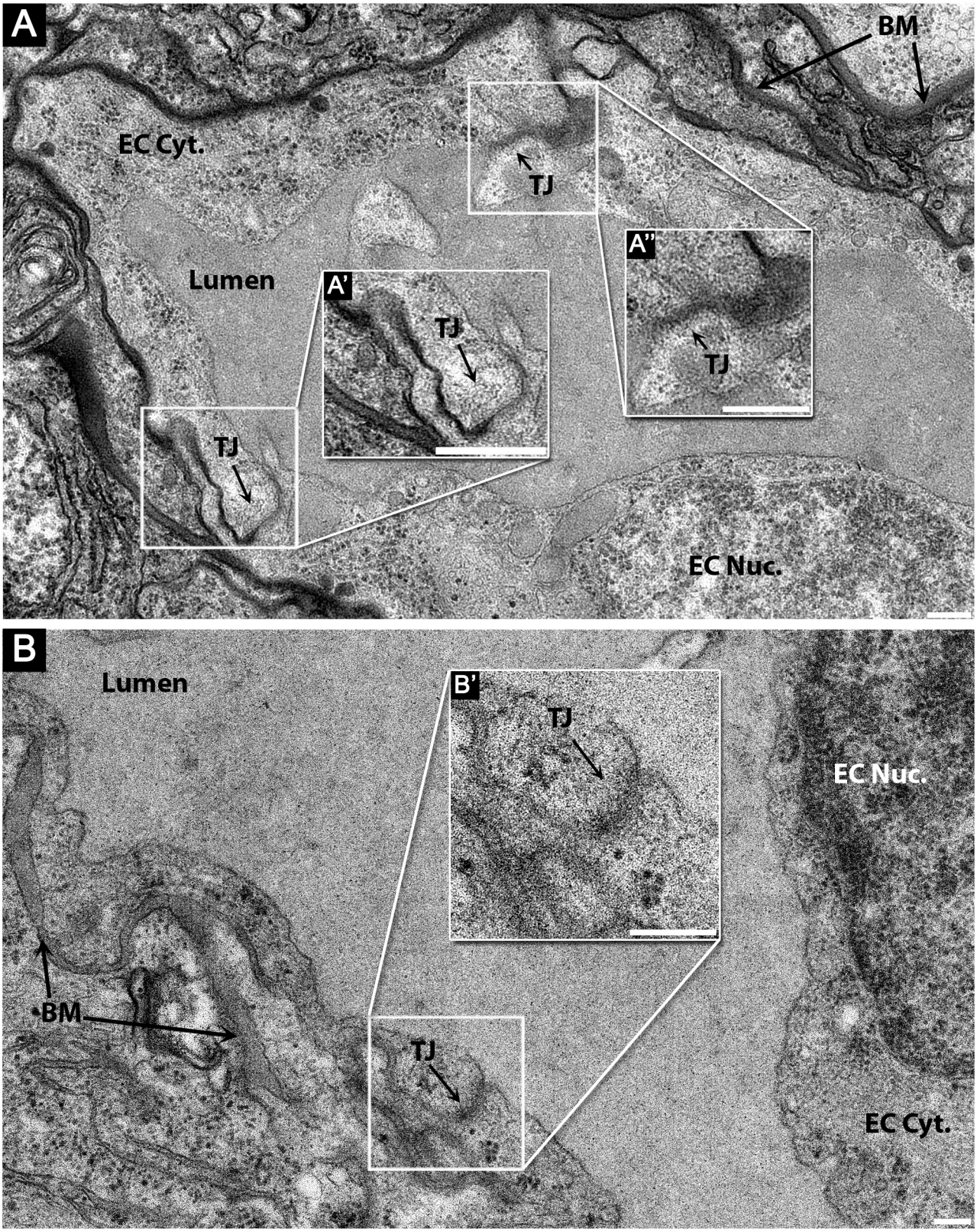

Figure S1. Zebrafish brain endothelia is not fenestrated.

(**A,B**) TEM images showing cross-section of brain blood capillaries containing tight junctions (TJ), dense basement membrane (BM) and lack fenestrae. (A', A''and B') Higher magnification of the tight junctions. EC cyto., endothelial cell cytoplasm; EC nuc., endothelial cell nucleus, Scale bars: 200 nm.


plvapa_[Danio_r
plvapb_[Danio_r
plvap_[Mus_musc
plvap_[Homo_sap
Identical residues
Similar residues
Transmembrane Domain
Coiled Coil Domain

Figure S2. Multiple sequence alignment for Plvap protein from zebrafish versus mammalian species.

Multiple sequence alignment of the deduced amino acids of zebrafish Plvap proteins (Plvapa_[Danio_r]] and (Plvapb_[Danio_r]] compared to mouse (plvap_[Mus_musc]) and human (plvap_[Homo_sap]) PLVAP proteins. Sequence alignment was generated by Clustal 2.1. The sequence identity/similarity between the species was analyzed by BoxShade 3.21. Black shading indicates sequence absolute identity, gray shading indicates sequence similarity. The transmembrane domain is highlighted by yellow, the coiled-coils are highlighted by red.

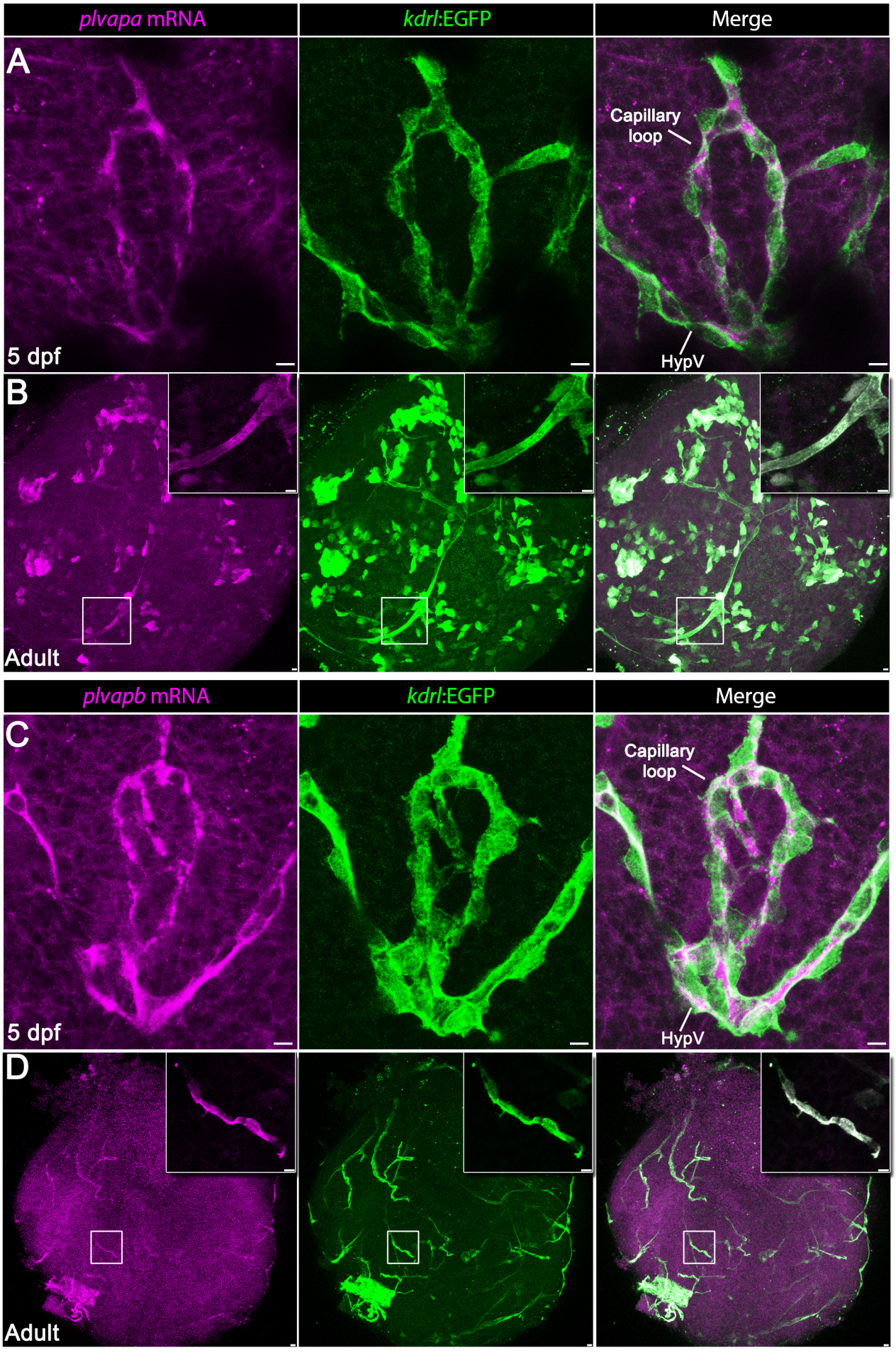

Figure S3. Zebrafish plvap orthologs expression is restricted to the hypophyseal vasculature.

(**A,B**) Whole-mount fluorescence in situ hybridization (FISH) of *plvapa* mRNA in a transgenic Tg(*kdrl*:EGFP) zebrafish larvae (5 dpf) (A) and adult hypophysis (B).

(**C,D**) Whole-mount fluorescence in situ hybridization (FISH) *plvapb* mRNA in a transgenic Tg(*kdrl*:EGFP) zebrafish larvae (5 dpf) (C) and adult hypophysis (D).

HypV, hypophyseal vein. Scale bars: 5 µm.

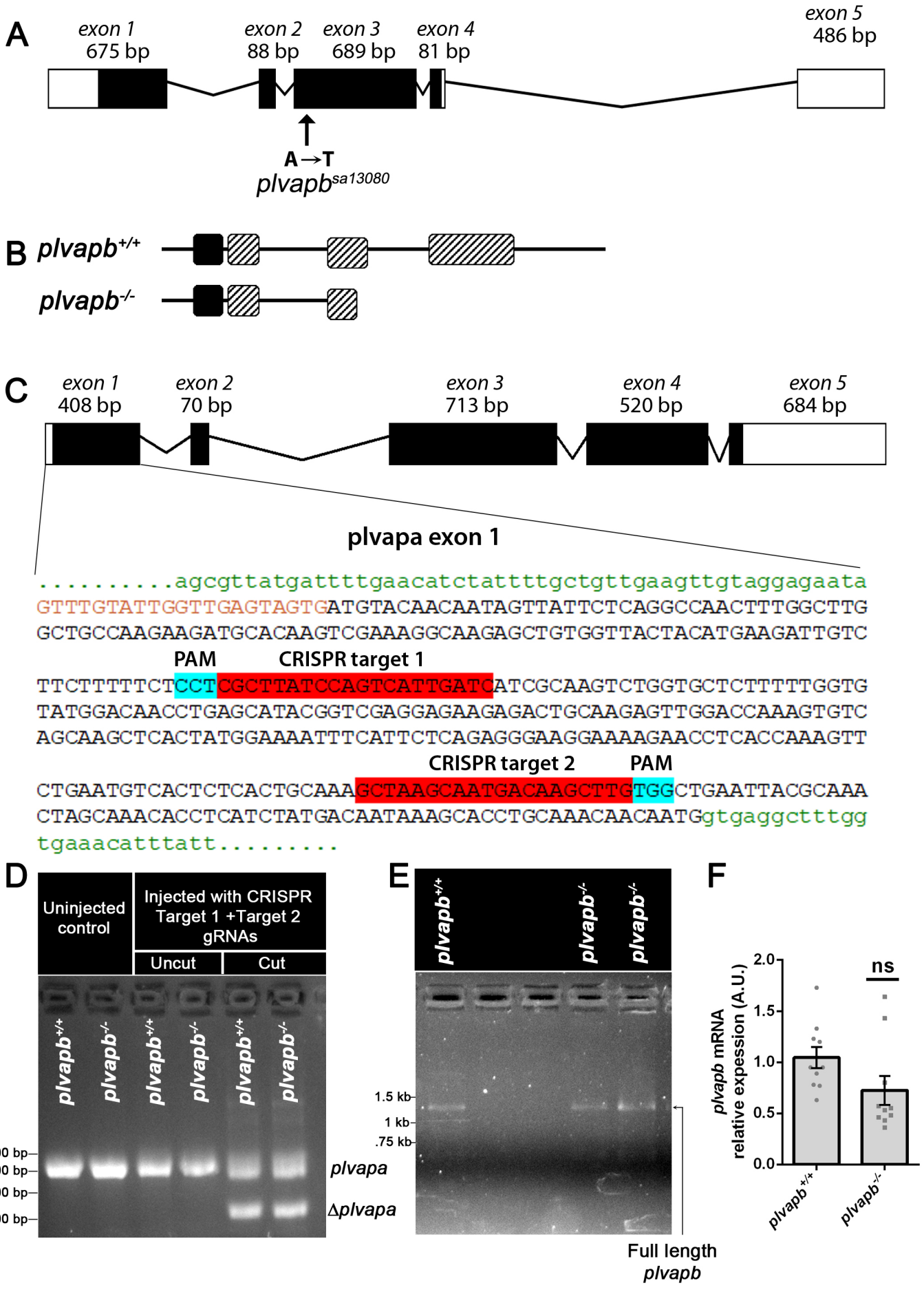

Figure S4. Characterization of *plvapa* and *plvapb* mutants.

(**A**) Schematic representation of the mutant *plvapb*^{sa13080} allele bearing a nonsense point mutation (A→T) in exon 3 of the zebrafish *plvapb* gene, replacing glutamine (a.a. 212) by a premature stop codon.

(**B**) Schematic representation of the predicted secondary structure of *plvapb*$^{+/+}$ and *plvapb*$^{-/-}$ proteins.

(**C**) Schematic representation of *plvapa* gene structure showing the nucleotide sequence of exon 1 and encoding the transmembrane domain and the position of two gRNAs binding sites as well as the forward and reverse genotyping primers.

(**D**) DNA gel electrophoresis showing PCR products of WT and mutant *plvapa* generated by CRISPR/Cas9 using gRNAs injected to an in-cross of heterozygous *plvapb*$^{+/-}$ fish resulting in deletion of 120 bp.

(**E**) DNA gel electrophoresis showing amplified PCR products of full length *plvapb* cDNA derived from *plvapb*$^{+/+}$ and *plvapb*$^{-/-}$ embryos.

(**F**) qRT-PCR analysis showing the relative expression of *plvapb* mRNA in *plvapb*$^{+/+}$ and *plvapb*$^{-/-}$. (ns=not significant; Student's *t*-test, n=10 for each genotype, A.U., arbitrary units). Data are presented as mean ± SEM.

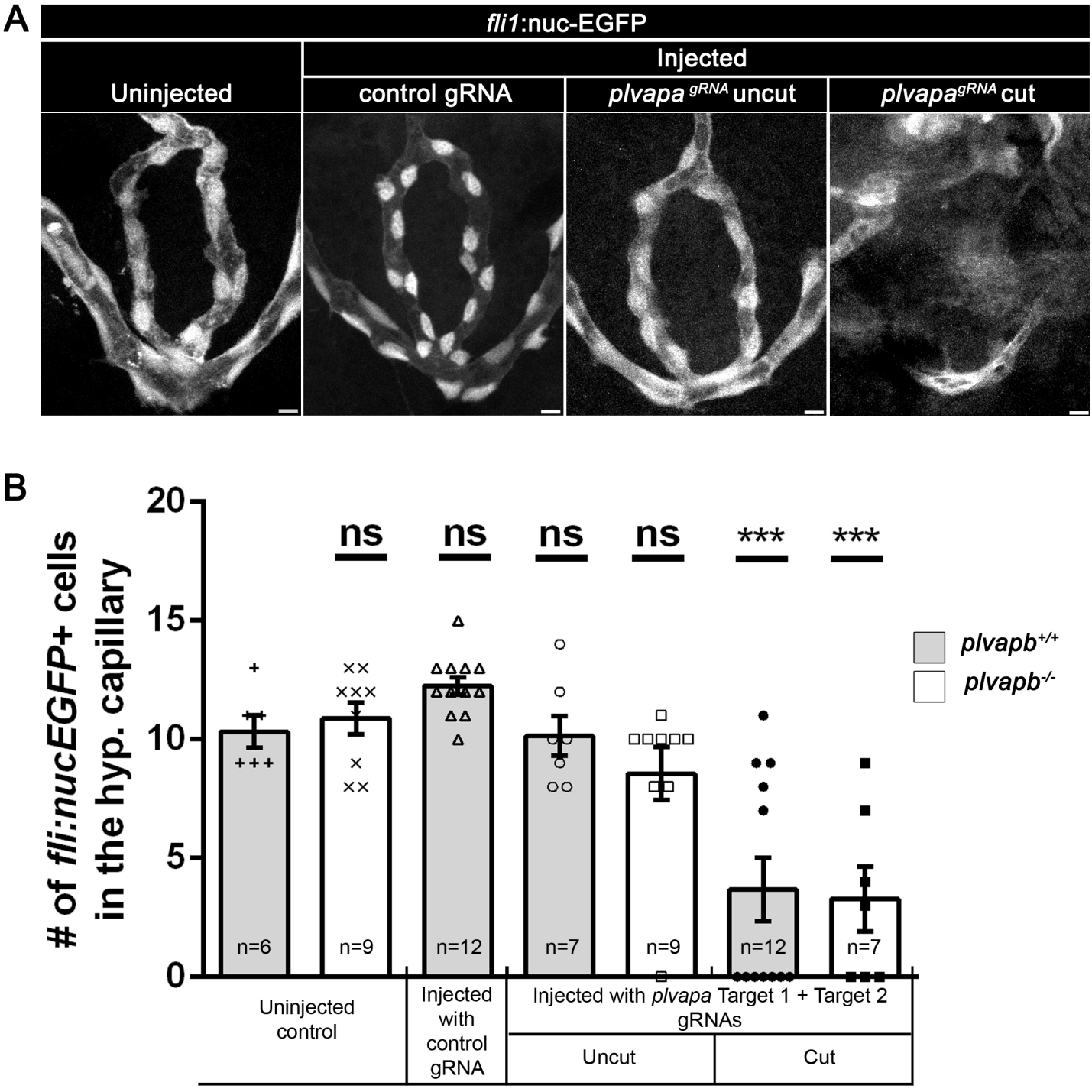

Figure S5. Deletion in *plvapa* gene significantly affects hypophyseal vascular morphology. (**A**) Confocal maximal projection images of Tg(*fli1*:nuc-EGFP) reporter line, showing the vascular hypophyseal capillary loop morphology and endothelial cell nuclei in transient *plvapa* crispant mutant.

(**B**) Quantification of the endothelial cell number in the vascular hypophyseal capillary loop of 5 dpf zebrafish Tg(*fli1*:nuc-EGFP) larvae. A transient *plvapa* crispant mutant was generated by simultaneous injection of two gRNAs (see Fig. S4) to an in-cross of heterozygous *plvapb*+/- fish, allowing the analysis of vascular morphology in single or double *plvapa/b* mutants. Larvae were genotyped for crispants bearing the expected *plvapa* deletion ("cut") or crispant in which no deletion was detected ("uncut"). A non-relevant control gRNA targeted to mCherry was used as mock crispant control. The injection of *plvapa* crispants to WT or *plvapb* mutant resulted in a significant loss of hypophyseal endothelial cells (***$p<0.001$, one-way ANOVA). A.U., arbitrary unit. Data are presented as mean ± SEM.

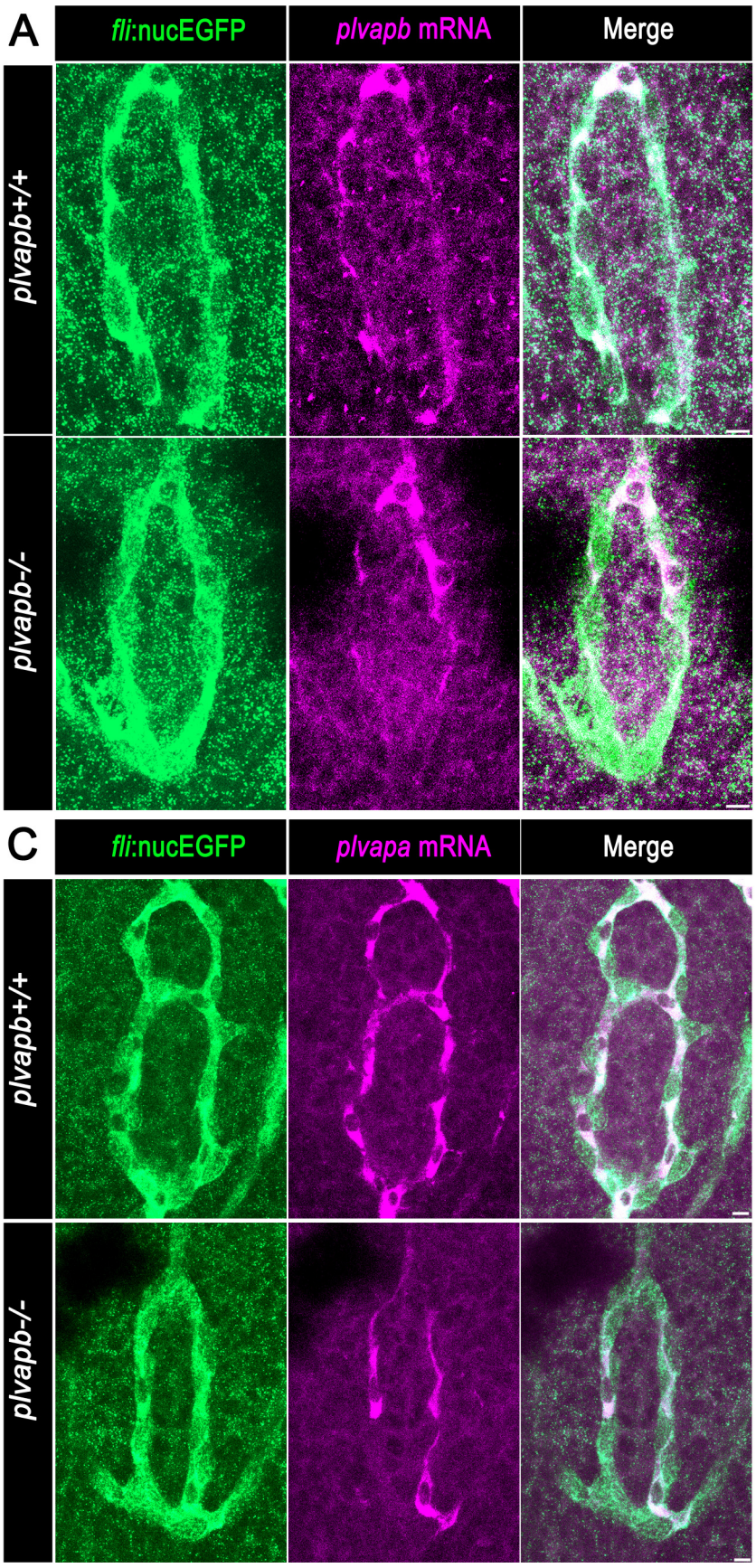

Figure S6. The effect of mutation in *plvapb* on the expression of *plvapa* and *plvapb* mRNA in the hypophyseal vasculature.

(A-D) Confocal maximal projection images of hypophyseal capillary loop in 5 dpf Tg(*fli1*:nucEGFP) larvae that were subjected to whole-mount fluorescence in situ hybridization (FISH) with RNA probes directed to *plvapb* (A) or *plvapa* (C) mRNAs. (B,D) Graphs showing respective mean fluorescent intensity of *plvapb* and *plvapa* in $plvapb^{+/+}$ and $plvapb^{-/-}$. (ns=not significant; *p<0.05; Student's *t*-test). Data are presented as mean ± SEM. Scale bars: 5 µm.

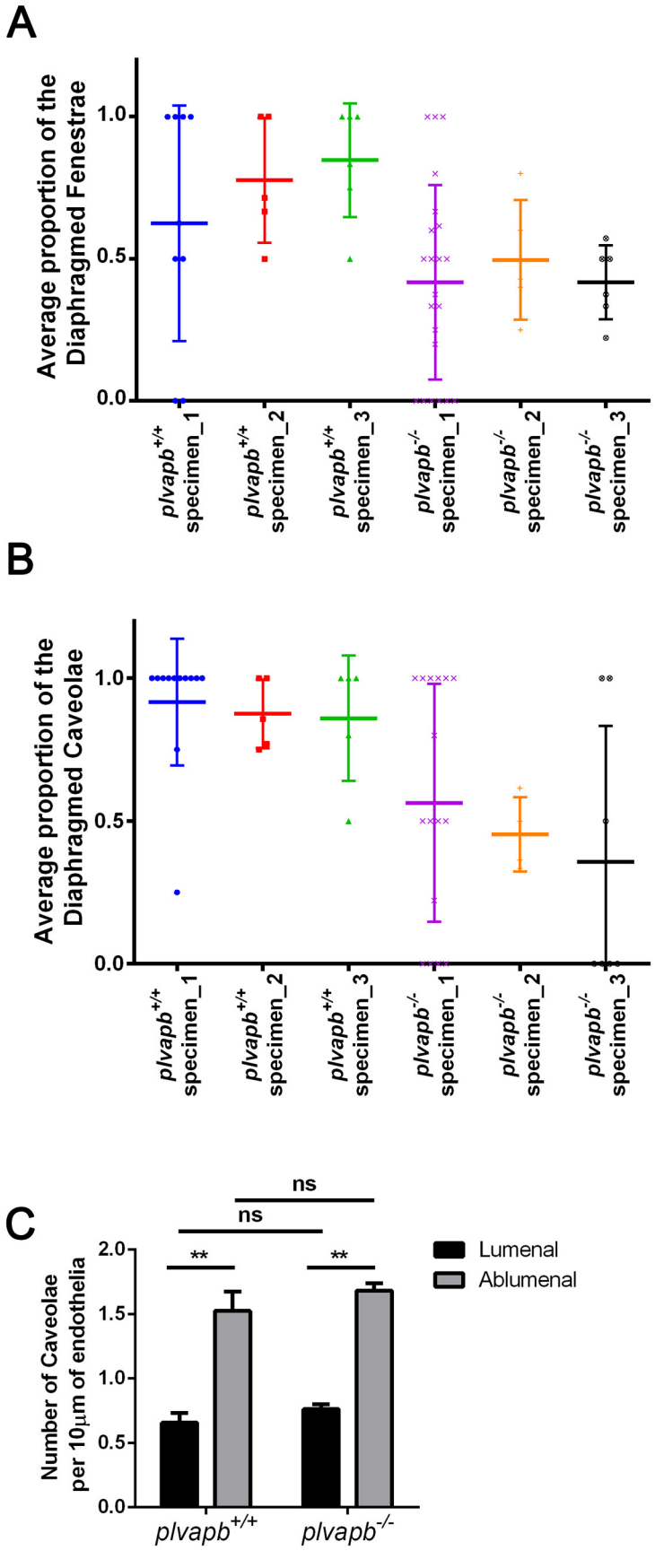

Figure S7. Quantification of diaphragmed fenestrae and caveolae in the hypophyseal endothelium of WT versus *plvapb*$^{-/-}$.

(A,B) Data showing average proportion of diaphragmed fenestrae (A) and caveolae (B) in all measured capillaries of individual biological repeats derived from *plvapb*$^{+/+}$ and *plvapb*$^{-/-}$ fish.

(C) Quantification of the linear density of abluminal and luminal caveolae per length unit of endothelium. The number of luminal and abluminal caveolae was counted and the endothelial cell length was measured within each blood capillary (5-25 blood capillaries per each biological repeat). The density was calculated as the number of luminal or abluminal caveolae divided by endothelial wall length (nm) and was thereafter multiplied by 10^4 to represent the result as density per 10 µm of endothelial wall. (**p<0.01, ns=not significant; two-way ANOVA, n=3 for each genotype). Data are presented as mean ± SEM.

Table S1 - KEY RESOURCES

REAGENT or RESOURCE	SOURCE	IDENTIFIER
Antibodies		
Mouse anti-Cldn5	ThermoFischer Scientific	35-2500
Alexa Fluor 647 anti-mouse, Secondary antibody	Jackson ImmunoResearch Laboratories (West Grove, PA).	115-605-003
Experimental Models: Organisms/Strains		
Tg(*oxtl*:EGFP)wz01	Gil Levkowitz Lab	ZFIN: ZDB-ALT-111103-1
Tg(*kdrl*:mCherry-caax)y171	Brant Weinstein Lab	ZFIN ID: ZDB-ALT-110429-3
Tg(*kdrl*:EGFP)s843	Didier Stainier Lab	ZFIN ID: ZDB-ALT-050916-14
Tg(*fli1a*:nucEGFP)y7	Brant Weinstein Lab	ZFIN ID: ZDB-FISH-150901-5696
Tg(*l-fabp*:DBP-EGFP)lri500	Bela Anand-Apte Lab	ZFIN ID: ZDB-ALT-120118-1
plvapb^{sa13080}	Sanger Institute Zebrafish Mutation Project	ZDB-ALT-130411-2744
Software and Algorithms		
ImageJ	NIH	
ImageJ FRAP Profiler tool	Jeff Hardin Lab	
Zen	Zeiss	
Photoshop CS6 Extended	Adobe	
SerialEM program	(Mastronarde, 2005)	
justblend script included in the IMOD software package	(Kremer et al., 1996)	

Table S2 related Figures 4, 5, 6, 7 and S3, S4, S5, S6, S7.

List of oligonucleotides used in this study

Gene	NCBI ID	*In situ* hybridization RNA probe synthesis		Quantitative Real Time PCR	
		Fwd	Rev	Fwd	Rev
plvapa	NM_001114577	AGGTTGAATAGTCAATGCGAGG	CTGGAGCAGTTGGAGCGAAT	CCCTCCCAAGCACAGGATTA	CCTAGTCCTGCTCCACCAAA
plvapb	NM_001030244	GCCAAGAAGATGCACAAGTCG	AATGGGCTAGTTCGCTTACAG	CTCCAAAGACCACACCAAAC	GCCTCGCATTGACTATTCAAC
Genotyping					
	Fwd		Rev		
plvapb^{sa13080}	ATGTGTCCACCAGCTAACCC		GCGAATCCTGTCCATCTGCT		
plvapa crispant	AAACTGGCAGCGTTATGATTTT		TTGACTGCTGTAGCATGCTTTG		
gRNAs used for CRISPR/Cas9 mediated mutagenesis					
gRNA	**Oligonucleotide Sequence**				
plvapa Target 1	GGTAATACGACTCACTATAGGTCAATGACTGGATAAGCGGTTTTAGAGCTAGAAATAGCAAG				
plvapa Target 2	GGTAATACGACTCACTATAGGTAAGCAATGACAAGCTTGGTTTTAGAGCTAGAAATAGCAAG				
mcherry Target 1	GGTAATACGACTCACTATAAGTAGTCGGGGATGTCGGCGGTTTTAGAGCTAGAAATAGCAAG				
mcherry Target 2	GGTAATACGACTCACTATAAGGCTGAAGCTGAAGGACGGGTTTTAGAGCTAGAAATAGCAAG				